Performance Analysis of Cooperative Spectrum Sensing for Cognitive Wireless Radio Networks over Nakagami-m Fading Channels

Quoc-Tuan Vien, Huan X. Nguyen, Ramona Trestian, Purav Shah, and Orhan Gemikonakli
School of Science and Technology, Middlesex University, The Burroughs, London NW4 4BT, UK.
Email: {q.vien; h.nguyen; r.trestian; p.shah; o.gemikonakli}@mdx.ac.uk.

***Abstract*—This paper is concerned with cooperative spectrum sensing (CSS) in cognitive wireless radio networks (CWRNs). A practical scenario is investigated where all channels suffer from Nakagami-m fading. Specifically, we analyse the probabilities of missed detection and false alarm for two CSS schemes where the collaboration is carried out either at fusion centre (FC) only or at both the FC and secondary user (SU). By deriving closed-form expressions and bounds of these probabilities, we not only show that there are significant impacts of the m-parameter of Nakagami fading realisation for different channel links on the sensing performance but also evaluate and compare the effectiveness of the two CSS schemes with respect to various fading parameters and the number of SUs. Finally, numerical results are provided to validate the theoretical analysis and findings.**

I. Introduction

Cognitive radio has been proposed as an emerging technology to cope with the scarcity of spectrum resource by implementing dynamic spectrum access [1]. In cognitive wireless radio networks (CWRNs), unlicenced users (or secondary users (SUs)) can opportunistically exploit unused licenced frequency bands of licenced users (or primary users (PUs)). Thus, the SUs should continuously sense the spectrum to check its availability. However, the implementation of spectrum sensing at SUs is limited for hidden terminal problems caused by shadowing and fading effects.

Recently, relay-assisted communications has been incorporated in various wireless systems (e.g. [2]–[4]). Data transmission from senders to receivers is carried out with the aid of relay terminals. The relays help improve service quality for near-by users and extend coverage region for far-end users. Adapting relaying techniques into CWRNs, cooperative spectrum sensing (CSS) has been then proposed not only to help the shadowed SUs detect the licenced frequency bands but also to improve sensing reliability of the SUs [5]–[7].

Specifically, a CSS scheme can be divided into three phases (e.g. in [7]) consisting of sensing (SS) phase, reporting (RP) phase, and backward (BW) phase. In the SS phase, every SU performs local spectrum sensing (LSS) to determine the availability of the licenced spectrum. Then, all SUs forward their local decisions to a common receiver, namely fusion centre (FC), in the RP phase. At the FC, a global spectrum sensing (GSS) is carried out to make a global decision on the spectrum availability, which is then broadcast back to all the SUs in the BW phase.

In this paper, we analyse the performance of CSS over Nakagami-m fading channels in terms of the probabilities of missed detection and false alarm. Given the LSS and GSS decisions available at the SUs, we consider two CSS schemes as follows: i) *Scheme 1*: The GSS decision is the final spectrum sensing (FSS) decision at the SUs (e.g. [6]) and ii) *Scheme 2*: Both the LSS and GSS decisions are taken into account to make the FSS decision at the SUs (e.g. [7]). Particularly, we investigate a practical scenario where all the SS, RP and BW channels suffer from fading and noise. This work is different from the published work which assumes either the RP or the BW channels are error-free [5], [6] or suffered from Rayleigh fading [7]. In this work, the fading channels are characterised by Nakagami-m distribution, which is used for modelling land-mobile and indoor-mobile multipath propagation [8], [9].

By deriving closed-form expressions of missed detection probability (MDP) and false alarm probability (FAP), we first compare the sensing performance achieved with the above CSS schemes. It is shown that the combination of GSS and LSS in scheme 2 results in a lower MDP compared to scheme 1, while it causes a higher FAP. Secondly, the effects of the number of SUs and the fading channel parameters are evaluated. Specifically, we derive the bounds of MDP and FAP when the number of SUs is large. Both schemes are shown to approach the same FAP and the bounds of MDP also show an improved performance achieved with scheme 2. Furthermore, the fading parameters of RP and BW channels are shown to have a significant impact on the sensing performance over those of SS channels.

II. System Model & Cooperative Spectrum Sensing

A. System Model

The system model of a CWRN under investigation is illustrated in Fig. 1 consisting of $\mathcal{PU}$, $\{\mathcal{SU}_1, \mathcal{SU}_2, \ldots, \mathcal{SU}_N\}$ and $\mathcal{FC}$. We assume there are K non-overlapping licenced frequency bands $f_1, f_2, \ldots, f_K$. For convenience, let us define a spectrum indicator vector (SIV) of length K (in bits) to report the availability of the licenced spectrum [7] where the unavailable and available frequency bands are represented by bits '0' and '1', respectively. The channel for a link $\mathcal{A} \rightarrow \mathcal{B}$,

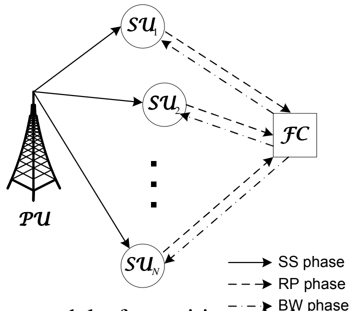

Fig. 1: System model of cognitive wireless relay network.

where $\{\mathcal{A}, \mathcal{B}\} \in \{\mathcal{PU}, \mathcal{SU}_1, \mathcal{SU}_2, \ldots, \mathcal{SU}_N, \mathcal{FC}\}$ and $\mathcal{A} \neq \mathcal{B}$, is denoted by h_{AB}[1] and assumed to suffer from quasi-static slow Nakagami-m fading.

B. Cooperative Spectrum Sensing (CSS)

In this subsection, let us briefly introduce three phases of CSS as follows:

1) Sensing (SS) Phase - Local Spectrum Sensing (LSS): Over the SS channel, the signal sensed at $\mathcal{SU}_i$, $i = 1, 2, \ldots, N$, at the k-th frequency band, $k = 1, 2, \ldots, K$, can be expressed as

$$\mathbf{r}_i^{(SS)}[k] = \begin{cases} h_{PS_i}\mathbf{x}[k] + \mathbf{n}_i^{(SS)}[k], & \mathcal{H}_{1,k}, \\ \mathbf{n}_i^{(SS)}[k], & \mathcal{H}_{0,k}, \end{cases} \tag{1}$$

where $\mathbf{x}[k]$ is the transmitted signal from $\mathcal{PU}$ and $\mathbf{n}_i^{(SS)}[k]$ is complex Gaussian noise at $\mathcal{SU}_i$ having zero mean and variance of σ_0^2. Here, $\mathcal{H}_{1,k}$ and $\mathcal{H}_{0,k}$ denote the two hypothesis that the k-th frequency band is occupied and unoccupied, respectively, by $\mathcal{PU}$. Then, $\mathcal{SU}_i$ detects the availability of the k-th frequency band by comparing the energy of the received signal in (1) with an energy threshold (denoted by $\varepsilon_i[k]$). Let $\mathbf{s}_i^{(L)}[k]$ denote the local SIV of the k-th frequency band estimated at $\mathcal{SU}_i$ and $\xi[\cdot]$ denote the energy measurement of a signal. We have

$$\mathbf{s}_i^{(L)}[k] = \begin{cases} 0, & \text{if } \xi[\mathbf{r}_i^{(SS)}[k]] \geqslant \varepsilon_i[k], \\ 1, & \text{otherwise.} \end{cases} \tag{2}$$

2) Reporting (RP) Phase - Global Spectrum Sensing (GSS): In RP phase, the received signal at $\mathcal{FC}$ from $\mathcal{SU}_i$, $i = 1, 2, \ldots, N$, at the k-th frequency band, $k = 1, 2, \ldots, K$, can be written by

$$\mathbf{r}_i^{(RP)}[k] = \sqrt{\Lambda_i} h_{S_iF}\mathbf{x}_i^{(LSS)}[k] + \mathbf{n}_i^{(RP)}[k], \tag{3}$$

where Λ_i is the transmission power of $\mathcal{SU}_i$, $\mathbf{x}_i^{(L)}[k]$ is the binary phase shift keying (BPSK) modulated version of $\mathbf{s}_i^{(L)}[k]$ (see (2)) and $\mathbf{n}_i^{(RP)}[k]$ is complex Gaussian noise at $\mathcal{FC}$ having zero mean and variance of σ_0^2. Then, $\mathcal{FC}$ decodes and combines all the decoded SIVs (denoted by $\{\mathbf{s}_i^{(RP)}[k]\}$) from all $\{\mathcal{SU}_i\}$ to make a global decision in terms of a global SIV as follows[2]:

$$\mathbf{s}_{FC}^{(G)}[k] = \begin{cases} 0, & \text{if } \sum_{i=1}^{N} \mathbf{s}_i^{(RP)}[k] < N, \\ 1, & \text{otherwise.} \end{cases} \tag{4}$$

[1]For brevity, A and B correspond the first letter of $\mathcal{PU}$, $\mathcal{SU}_i$ and $\mathcal{FC}$ (i.e. P, S_i, F).

[2]The OR rule is used since it was shown to give the best CSS performance compared to other rules [10].

3) Backward (BW) Phase - Final Spectrum Sensing (FSS): The received signal at $\mathcal{SU}_i$, $i = 1, 2, \ldots, N$, from $\mathcal{FC}$ with respect to the k-th frequency band, $k = 1, 2, \ldots, K$, can be written by

$$\mathbf{r}_i^{(BW)}[k] = \sqrt{\Lambda_{FC}} h_{FS_i}\mathbf{x}_{FC}^{(G)}[k] + \mathbf{n}_i^{(BW)}[k], \tag{5}$$

where Λ_{FC} is the transmission power of $\mathcal{FC}$, $\mathbf{x}_{FC}^{(G)}[k]$ is the BPSK modulated version of $\mathbf{s}_{FC}^{(G)}[k]$ (see (4)) and $\mathbf{n}_i^{(BW)}[k]$ is complex Gaussian noise at $\mathcal{SU}_i$ over the BW channel having zero mean and variance of σ_0^2. Then, $\mathcal{SU}_i$ decodes the received signal as $\mathbf{s}_i^{(BW)}[k]$. Let us denote $\mathbf{s}_i^{(F_j)}[k]$ as the final SIV of the k-th frequency band, $k = 1, 2, \ldots, K$, at $\mathcal{SU}_i$, $i = 1, 2, \ldots, N$, using scheme j, $j = 1, 2$ (as described in Section I).

<u>*Scheme 1 - Non-combined scheme*</u>: In this scheme, the GSS decision received from $\mathcal{FC}$ is also the final decision at $\mathcal{SU}_i$. Thus, we simply have

$$\mathbf{s}_i^{(F_1)}[k] = \mathbf{s}_i^{(BW)}[k]. \tag{6}$$

<u>*Scheme 2 - Combined scheme*</u>: In this scheme, $\mathcal{SU}_i$ combines its local SIV with the global SIV received from $\mathcal{FC}$ as follows [7]:

$$\mathbf{s}_i^{(F_2)}[k] = \begin{cases} 0, & \text{if } (\mathbf{s}_i^{(L)}[k] + \mathbf{s}_i^{(BW)}[k]) < 2, \\ 1, & \text{otherwise.} \end{cases} \tag{7}$$

III. Performance Analysis

In this section, we derive closed-form expressions and bounds for the false alarm probability (FAP) and the missed detection probability (MDP) of CSS schemes in CWRNs over Nakagami-m fading channels.

Definition 1. The FAP and MDP of the k-th frequency band (i.e. f_k), $k = 1, 2, \ldots, K$, at node $\mathcal{A}$, $\mathcal{A} \in \{\mathcal{SU}_i, \mathcal{FC}\}$, $i = 1, 2, \ldots, N$, using scheme j, $j = 1, 2$, are defined as

$$P_{f,j}^{(SU_i)} \triangleq Pr\{\mathbf{s}_i^{(M_j)}[k] = 0 | \mathcal{H}_{0,k}\}, \tag{8}$$

$$P_{m,j}^{(SU_i)} \triangleq Pr\{\mathbf{s}_i^{(M_j)}[k] = 1 | \mathcal{H}_{1,k}\}, \tag{9}$$

respectively, where $M \in \{L, G, F\}$.

The Nakagami fading parameters of the SS, RP and BW channels are denoted by m_{ss}, m_{rp} and m_{bw}, respectively. For simplicity, let us assume that the RP and BW channels of the same link have the same Nakagami fading parameters (i.e. $m_{rp} = m_{bw}$) and all the SUs have the same energy threshold for detection of the k-th frequency band (i.e. $\varepsilon_i[k] = \varepsilon[k]$ $\forall i = 1, 2, \ldots, N$)[3]. Without loss of generality, we analyse the performance for a specific frequency band and thus the index of the frequency band (i.e. k) is omitted in the rest of the paper.

Let us first consider the LSS at $\mathcal{SU}_i$, $i = 1, 2, \ldots, N$. Define $\alpha \triangleq \varepsilon/(2\sigma_0^2)$, $\beta_i \triangleq m_{ss}\sigma_0^2/(m_{ss}\sigma_0^2 + \gamma_{PS_i})$, where γ_{PS_i} is the average signal-to-noise ratio (SNR) at $\mathcal{SU}_i$ over h_{PS_i}. The FAP and MDP of the LSS are given by [11]

$$P_f^{(SU_i)} = \Pr\{s_i^{(L)} = 0 | \mathcal{H}_0\} = \frac{\Gamma_u(\rho, \alpha)}{\Gamma(\rho)}, \tag{10}$$

[3]The performance analysis for the general scenario of various fading parameters and energy thresholds can be easily extended by aggregating the performance achieved at SUs over the associated RP and BW links.

$$P_m^{(SU_i)} = \Pr\{s_i^{(L)} = 1|\mathcal{H}_1\} = 1 - \vartheta_{i,1} - \vartheta_{i,2}, \quad (11)$$

where

$$\vartheta_{i,1} = e^{\left(-\frac{\alpha\beta_i}{m_{ss}}\right)}[\beta_i^{m_{ss}-1} L_{m_{ss}-1}(-\alpha(1-\beta_i)) + (1-\beta_i)\sum_{j=0}^{m_{ss}-2} \beta_i^j L_j(-\alpha(1-\beta_i))], \quad (12)$$

$$\vartheta_{i,2} = \beta_i^{m_{ss}} e^{-\alpha} \sum_{j=1}^{\rho-1} \frac{\alpha^j}{j!} {}_1F_1(m_{ss}; j+1; \alpha(1-\beta_i)), \quad (13)$$

ρ denotes the time-bandwidth product of the energy detector, $\Gamma(\cdot)$ is the gamma function [12, eq. (8.310.1)], $\Gamma_u(\cdot,\cdot)$ is the upper incomplete gamma function [12, eq. (8.350.2)], ${}_1F_1(\cdot;\cdot;\cdot)$ is the confluent hypergeometric function [12, eq. (9.210.1)] and $L_i(\cdot)$ is the Laguerre polynomial of degree i [12, eq. (8.970.2)].

Note that over a Nakagami-m fading channel h_{AB}, the average bit error rate (BER) for BPSK modulation with respect to the average SNR of γ_{AB} is obtained as in [13] and given below

$$P_b(E_{AB}) = \left(1 + \frac{\gamma_{AB}}{m_{AB}}\right)^{-m_{AB}} \frac{\Gamma(m_{AB}+1/2)}{2\sqrt{\pi}\Gamma(m_{AB}+1)} \times {}_2F_1(m_{AB}, 1/2; m_{AB}+1; 1/(1+\gamma_{AB}/m_{AB})), \quad (14)$$

where ${}_2F_1(\cdot,\cdot;\cdot;\cdot)$ is the Gauss hypergeometric function [12, eq. (9.100)]. For brevity, let us define a function $\psi(m_{AB}, \gamma_{AB})$ (or ψ_{AB} in short) as the RHS of (14).

Considering the GSS at $\mathcal{FC}$ over the RP channels suffered from Nakagami-m fading, we have the following finding:

Lemma 1. *The FAP and MDP of the GSS are determined by*

$$P_f^{(FC)} = 1 - \frac{1}{[\Gamma(\rho)]^N} \prod_{i=1}^{N} [\Gamma_l(\rho,\alpha)(1-\psi_{S_iF}) + \Gamma_u(\rho,\alpha)\psi_{S_iF}], \quad (15)$$

$$P_m^{(FC)} = \prod_{i=1}^{N} [(1-\vartheta_{i,1}-\vartheta_{i,2})(1-\psi_{S_iF}) + (\vartheta_{i,1}+\vartheta_{i,2})\psi_{S_iF}], \quad (16)$$

where ψ_{S_iF} is given by (14) *and $\Gamma_l(\cdot,\cdot)$ is the lower incomplete gamma function [12, eq. (8.350.1)].*

Proof: From (4), the FAP and MDP at $\mathcal{FC}$ can be given by

$$P_f^{(FC)} = \Pr\{s_{FC}^{(G)} = 0|\mathcal{H}_0\} = 1 - \prod_{i=1}^{N} \Pr\{s_i^{(RP)} = 1|x=0\}, \quad (17)$$

$$P_m^{(FC)} = \Pr\{s_{FC}^{(G)} = 1|\mathcal{H}_1\} = \prod_{i=1}^{N} \Pr\{s_i^{(RP)} = 1|x \neq 0\}, \quad (18)$$

where x is the transmitted signal from $\mathcal{PU}$. Thus, over the Nakagami-m fading channels $\{h_{S_iF}\}$, $i = 1,2,\ldots,N$, with BER of ψ_{S_iF} (see (14)), we have

$$P_f^{(FC)} = 1 - \prod_{i=1}^{N} [(1-P_f^{(SU_i)})(1-\psi_{S_iF}) + P_f^{(SU_i)}\psi_{S_iF}], \quad (19)$$

$$P_m^{(FC)} = \prod_{i=1}^{N} [P_m^{(SU_i)}(1-\psi_{S_iF}) + (1-P_m^{(SU_i)})\psi_{S_iF}]. \quad (20)$$

Substituting (10) and (11) into (19) and (20) with the fact $\Gamma_u(\rho,\alpha) + \Gamma_l(\rho,\alpha) = \Gamma(\rho)$ [12, eq. (8.356.3)], the lemma is proved. ■

In the BW phase, the FSS at $\mathcal{SU}_i$, $i = 1,2,\ldots,N$, is carried out using either of two schemes, namely non-combined and combined schemes (see Sect. II-B.3). We then have the following findings:

Lemma 2. *The FAP and MDP of the FSS at $\mathcal{SU}_i$, $i = 1,2,\ldots,N$, using scheme 1 are determined by*

$$P_{f,1}^{(SU_i)} = 1 - [(1-P_f^{(FC)})(1-\psi_{FS_i}) + P_f^{(FC)}\psi_{FS_i}], \quad (21)$$

$$P_{m,1}^{(SU_i)} = P_m^{(FC)}(1-\psi_{FS_i}) + (1-P_m^{(FC)})\psi_{FS_i}, \quad (22)$$

where ψ_{FS_i}, $P_f^{(FC)}$ and $P_m^{(FC)}$ are given by (14), (15) *and* (16)*, respectively.*

Proof: In scheme 1, the FSS at $\mathcal{SU}_i$, $i = 1,2,\ldots,N$, is also the GSS feedback from $\mathcal{FC}$ over the Nakagami-m BW channels $\{h_{FS_i}\}$. Following the same approach as in the proof of Lemma 1, $P_{f,1}^{(SU_i)}$ and $P_{m,1}^{(SU_i)}$ can be calculated by (21) and (22), respectively. ■

Lemma 3. *The FAP and MDP of the FSS at $\mathcal{SU}_i$, $i = 1,2,\ldots,N$, using scheme 2 are determined by*

$$P_{f,2}^{(SU_i)} = 1 - \frac{1}{\Gamma(\rho)}[\Gamma_l(\rho,\alpha)(1-\psi_{FS_i}) + \Gamma_u(\rho,\alpha)\psi_{FS_i}] \times [(1-P_f^{(FC)})(1-\psi_{FS_i}) + P_f^{(FC)}\psi_{FS_i}], \quad (23)$$

$$P_{m,2}^{(SU_i)} = [(1-\vartheta_{i,1}-\vartheta_{i,2})(1-\psi_{FS_i}) + (\vartheta_{i,1}+\vartheta_{i,2})\psi_{FS_i}] \times [P_m^{(FC)}(1-\psi_{FS_i}) + (1-P_m^{(FC)})\psi_{FS_i}], \quad (24)$$

where ψ_{FS_i}, $P_f^{(FC)}$ and $P_m^{(FC)}$ are given by (14), (15) *and* (16)*, respectively.*

Proof: In scheme 2, the FSS at $\mathcal{SU}_i$, $i = 1,2,\ldots,N$, is obtained by combining both the GSS from $\mathcal{FC}$ and the LSS. From (7), $P_{f,2}^{(SU_i)}$ and $P_{m,2}^{(SU_i)}$ can be given by

$$P_{f,2}^{(SU_i)} = \Pr\{s_i^{(F_2)} = 0|\mathcal{H}_0\} = 1 - \Pr\{s_i^{(L)} = 1|x=0\}\Pr\{s_i^{(BW)} = 1|x=0\}, \quad (25)$$

$$P_{m,2}^{(SU_i)} = \Pr\{s_i^{(F_2)} = 1|\mathcal{H}_1\} = \Pr\{s_i^{(L)} = 1|x \neq 0\}\Pr\{s_i^{(BW)} = 1|x \neq 0\}. \quad (26)$$

where x is the transmitted signal from $\mathcal{PU}$. Thus, over the Nakagami-m BW channels h_{FS_i} with BER of ψ_{FS_i}, $P_{f,2}^{(SU_i)}$ and $P_{m,2}^{(SU_i)}$ can be obtained by (23) and (24), respectively. ■

Remark 1 (*Lower FAP with Scheme 1 and Lower MDP with Scheme 2*)**.** From (21), (22), (23) and (24) in Lemmas 2 and 3, it can be easily shown that $P_{f,1}^{(SU_i)} < P_{f,2}^{(SU_i)}$ and $P_{m,1}^{(SU_i)} > P_{m,2}^{(SU_i)}$, $i = 1,2,\ldots,N$. This accordingly means a lower FAP is achieved with scheme 1 compared to scheme 2, while scheme 2 achieves a lower MDP than scheme 1.

Remark 2 (*Lower MDP but Higher FAP with Increased Number of SUs*)**.** Both CSS schemes improve the MDP but cause higher FAP at SUs when the number of SUs increases. From (15) and (16) in Lemma 1, it can be seen that $P_f^{(FC)}$ and $P_m^{(FC)}$ monotonically increase and decrease, respectively, over N. Thus, from (21), (22), (23) and (24), the increased number of SUs helps both CSS schemes improve the MDP, however, causing a higher FAP.

Remark 3 (*Impact of Nakagami-m Fading Parameters on MDP and FAP*)**.** Both the MDP and FAP decrease when the fading parameters of RP and BW channels increase, while only MDP is improved with increased fading parameters of SS channels. In fact, it is known that the BER of a Nakagami-m fading channel h_{AB} monotonically decreases as m_{AB} increases (see (14)). Thus, from (21), (22), (23) and (24), it can be proved that $P_{f,j}^{(SU_i)}$ and $P_{m,j}^{(SU_i)}$, $i = 1, 2, \ldots, N$, $j = 1, 2$, monotonically decrease as either m_{rp} or m_{bw} increases. Additionally, as shown in (10) and (11), $P_f^{(SU_i)}$, $i = 1, 2, \ldots, N$, of the LSS is independent of m_{ss}, while a lower $P_m^{(SU_i)}$ is achieved as m_{ss} increases. This accordingly results in an invariant final FAP $P_{f,j}^{(SU_i)}$, $i = 1, 2, \ldots, N$, $j = 1, 2$, over m_{ss}, but a lower final MDP $P_{m,j}^{(SU_i)}$ is achieved with the increased m_{ss}.

Bounds of FAPs and MDPs:

According to Remark 2, there is a significant impact of the number of SUs on FAPs and MDPs of two CSS schemes in CWRNs. For the sake of providing insightful meanings of the above derived expressions for the FAPs and MDPs of the two CSS schemes, let us investigate a specific scenario of identical channels, i.e. $\gamma_{PS_i} \triangleq \gamma_{ss}$, $\gamma_{S_iF} \triangleq \gamma_{rp}$, $\gamma_{FS_i} \triangleq \gamma_{bw}$, $\forall i = 1, 2, \ldots, N$. Thus, from (12) and (13), we can rewrite $\vartheta_{i,1} = \vartheta_1$ and $\vartheta_{i,2} = \vartheta_2$. We then have the following findings:

Lemma 4. *When the number of SUs is very large, i.e. $N \to \infty$, FAP and MDP of scheme 1 approach $P_{f,1_{N_\infty}}^{(SU)}$ and $P_{m,1_{N_\infty}}^{(SU)}$, respectively, where*

$$P_{f,1_{N_\infty}}^{(SU)} = 1 - \psi_{bw}, \quad (27)$$

$$P_{m,1_{N_\infty}}^{(SU)} = \psi_{bw}. \quad (28)$$

Proof: As $N \to \infty$, from Lemma 1, it can be seen that $P_f^{(FC)} \to 1$ and $P_m^{(FC)} \to 0$. Substituting into (21) and (22), we obtain $P_{f,1_{N_\infty}}^{(SU)}$ and $P_{m,1_{N_\infty}}^{(SU)}$ as shown in (27) and (28). ■

Lemma 5. *When the number of SUs is very large, i.e. $N \to \infty$, FAP and MDP of scheme 2 approach $P_{f,2_{N_\infty}}^{(SU)}$ and $P_{m,2_{N_\infty}}^{(SU)}$, respectively, where*

$$P_{f,2_{N_\infty}}^{(SU)} = 1 - \frac{\Gamma_l(\rho, \alpha)}{\Gamma(\rho)} \psi_{bw} - \frac{\Gamma_u(\rho, \alpha) - \Gamma_l(\rho, \alpha)}{\Gamma(\rho)} \psi_{bw}^2, \quad (29)$$

$$P_{m,2_{N_\infty}}^{(SU)} = (1 - \vartheta_1 - \vartheta_2)\psi_{bw} - (1 - 2\vartheta_1 - 2\vartheta_2)\psi_{bw}^2. \quad (30)$$

Proof: Similar to the proof of Lemma 4, we substitute $P_f^{(FC)} \to 1$ and $P_m^{(FC)} \to 0$ into (23) and (24), and thus obtain $P_{f,2_{N_\infty}}^{(SU)}$ and $P_{m,2_{N_\infty}}^{(SU)}$ as shown in (29) and (30). ■

Remark 4 (*Lower MDP Bound with Scheme 2 and Approximately Similar FAP Bounds*)**.** In fact, from (28) and (30), it can be easily shown that $P_{m,2_{N_\infty}}^{(SU)} < P_{m,1_{N_\infty}}^{(SU)}$, which means a lower MDP bound is achieved with scheme 2. Considering the FAP bound, it is noted that $\Gamma_l(\rho, \alpha) \approx \Gamma(\rho)$ as $\alpha = \varepsilon/(2\sigma_0^2) \to \infty$. Also, we have $\psi_{bw}^2 \ll \psi_{bw} < 1$. Thus, from (29), we have $P_{f,2_{N_\infty}}^{(SU)} \approx 1 - \psi_{bw} = P_{f,1_{N_\infty}}^{(SU)}$. This accordingly means that both schemes approach the same FAP bound as the number of SUs is very large.

IV. Numerical Results

In this section, we evaluate the FAP and MDP performance of CSS schemes in CWRNs, including

- *Scheme 1 - Non-combined scheme*: There is no combination of decisions at the SUs over BW links.
- *Scheme 2 - Combined scheme*: There is a binary combination of decisions at the SUs over BW links.

Specifically, the analytical formulations derived for the FAP and MDP of the above two CSS schemes as well as observations deduced in the previous section are now discussed and validated.

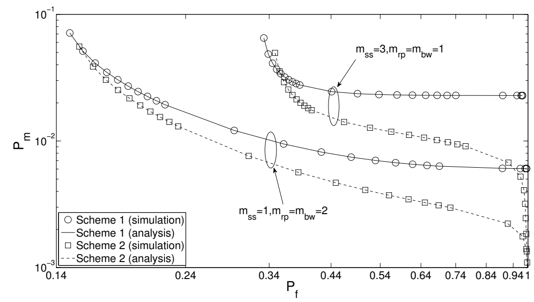

Fig. 2: Performance comparison of two CSS schemes.

Fig. 2 shows the MDP against the FAP of two CSS schemes with respect to various fading parameters and various values of the energy threshold. We assume there are 10 SUs (i.e. $N = 10$) and the time-bandwidth product of the energy detector is $\rho = 5$. The SNRs of the channels are set as follows: $\{\gamma_{PS_i}\} = \{10, 8, 9, 12, 5, 7, 8, 4, 2, 6\}$ dB, $\{\gamma_{S_iF}\} = \{8, 7, 10, 4, 6, 8, 9, 11, 8, 10\}$ dB and $\{\gamma_{FS_i}\} = \{10, 11, 13, 9, 8, 14, 11, 10, 12, 7\}$ dB. Two Nakagami-m fading scenarios (NFSs) are considered: i) $m_{ss} = 3$, $m_{rp} = m_{bw} = 1$ and ii) $m_{ss} = 1$, $m_{rp} = m_{bw} = 2$. It can be observed in Fig. 2 that, at a given energy threshold in either NFS, scheme 2 achieves a lower MDP than scheme 1, while a lower FAP is achieved with scheme 1 compared to scheme 2. This observation confirms the statement in Remark 1 regarding the lower FAP with scheme 1 and the lower MDP with scheme 2. Additionally, in Fig. 2, the analytical results of the FAP and MDP for both CSS schemes derived in Lemmas 2 and 3 are shown to be consistent with the simulation results.

Investigating the impact of Nakagami-m fading parameters on the sensing performance of the CSS, Fig. 3 plots the MDP versus FAP of scheme 2 with respect to various NFSs[4]:

- (NFS1): $m_{ss} = 1$, $m_{rp} = m_{bw} = 1$
- (NFS2): $m_{ss} = 1$, $m_{rp} = m_{bw} = 2$
- (NFS3): $m_{ss} = 2$, $m_{rp} = m_{bw} = 1$

[4]The impact of the fading parameters on the sensing performance of scheme 1 can be similarly observed, and thus is omitted for brevity.

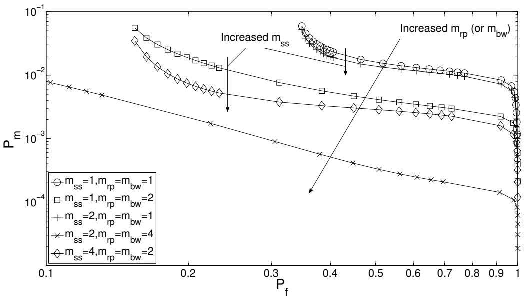

Fig. 3: Performance of CSS scheme 2 with various NFSs.

- (NFS4): $m_{ss} = 2$, $m_{rp} = m_{bw} = 4$
- (NFS5): $m_{ss} = 4$, $m_{rp} = m_{bw} = 2$

A total of 10 SUs is considered and the SNRs of the SS, RP and BW channels are similarly set as in Fig. 2. Let us first evaluate the impact of RP and BW channel parameters. As shown in Fig. 3, given fixed m_{ss} (e.g. (NFS1) vs (NFS2) or (NFS3) vs (NFS4)), both the MDP and FAP are improved as m_{rp} (or m_{bw}) increases. Considering the scenario of fixed m_{rp} and m_{bw} (e.g. (NFS1) vs (NFS3) or (NFS2) vs (NFS5)), it can be observed that only a lower MDP is achieved as m_{ss} increases, while the FAP is unchanged for all values of the energy threshold. These above comparisons verify the statement in Remark 3 regarding the impact of the Nakagami-m fading parameters of the SS, RP and BW channels on the sensing performance.

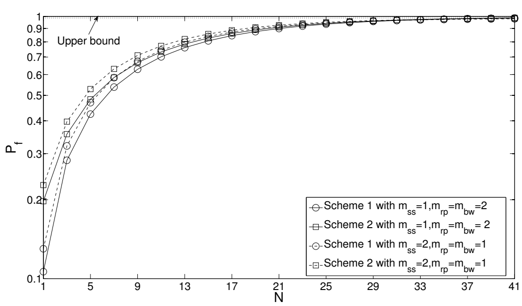

Fig. 4: FAP of CSS schemes over the number of SUs.

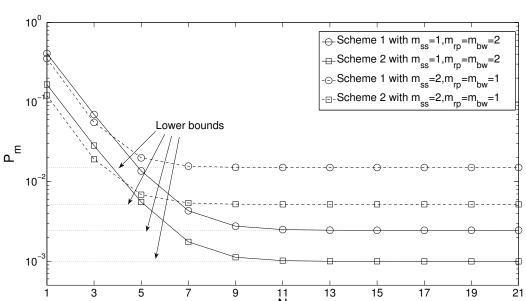

Fig. 5: MDP of CSS schemes over the number of SUs.

Taking into consideration the impact of the number of SUs on the sensing performance of various CSS schemes, as shown in Figs. 4 and 5, the FAP and MDP of the two aforementioned CSS schemes are plotted as functions of the number of SUs (i.e. N). The SNRs of the SS, RP and BW links are set as 8 dB, 10 dB and 12 dB, respectively. We consider two NFSs: i) $m_{ss} = 1$, $m_{rp} = m_{bw} = 2$ and ii) $m_{ss} = 2$, $m_{rp} = m_{bw} = 1$. It can be observed in Figs. 4 and 5 that both schemes approach the similar FAP upper bound as N is large, while the MDP of scheme 2 approaches a lower MDP bound in both NFSs. This accordingly verifies the statements in Remarks 2 and 4 about the MDP lower bound and the FAP upper bound with a large number of SUs. Additionally, the FAP and MDP of the two CSS schemes are shown to approach the bounds given by (27), (28), (29) and (30) in Lemmas 4 and 5.

V. Conclusions

In this paper, we have analysed the sensing performance of two CSS schemes for CWRNs considering the practical scenario where all SS, RP and BW channels suffer from Nakagami-m fading and background noise. The combined CSS scheme (scheme 2) has been shown to achieve an improved MDP while causing a higher FAP when compared to the non-combined CSS scheme (scheme 1). As the number of SUs is very large, the performance bounds have shown that both schemes approach the similar FAP upper bound and the MDP lower bound of the combined scheme is still smaller than that of the non-combined scheme. Furthermore, the derived expressions reflect well the impact of the Nakagami-m fading parameters of various links on the sensing performance. Both the MDP and FAP are improved as the fading parameters of the RP and BW channels increase, while the increased fading parameters of SS channels only results in a lower MDP.

References

[1] S. Haykin, "Cognitive radio: brain-empowered wireless communications," *IEEE J. Sel. Areas Commun.*, vol. 23, no. 2, pp. 201–220, Feb. 2005.

[2] K. Loa, C.-C. Wu, S.-T. Sheu, Y. Yuan, M. Chion, D. Huo, and L. Xu, "IMT-advanced relay standards [WiMAX/LTE update]," *IEEE Commun. Mag.*, vol. 48, no. 8, pp. 40–48, Aug. 2010.

[3] S. Sharma, Y. Shi, Y. Hou, and S. Kompella, "An optimal algorithm for relay node assignment in cooperative ad hoc networks," *IEEE/ACM Trans. Netw.*, vol. 19, no. 3, pp. 879–892, Jun. 2011.

[4] Q.-T. Vien, H. X. Nguyen, O. Gemikonakli, and B. Barn, "Performance analysis of cooperative transmission for cognitive wireless relay networks," in *Proc. IEEE GLOBECOM 2013*, Atlanta, Georgia, USA, Dec. 2013, pp. 4186–4191.

[5] G. Ganesan and Y. Li, "Cooperative spectrum sensing in cognitive radio, part I: Two user networks," *IEEE Trans. Wireless Commun.*, vol. 6, no. 6, pp. 2204–2213, Jun. 2007.

[6] W. Zhang and K. Letaief, "Cooperative spectrum sensing with transmit and relay diversity in cognitive radio networks," *IEEE Trans. Wireless Commun.*, vol. 7, no. 12, pp. 4761–4766, Dec. 2008.

[7] Q.-T. Vien, H. Tianfield, and B. G. Stewart, "Efficient cooperative spectrum sensing for cognitive wireless relay networks over Rayleigh flat fading channels," in *Proc. IEEE VTC 2012-Spring*, Yokohama, Japan, May 2012, pp. 1–5.

[8] W. Braun and U. Dersch, "A physical mobile radio channel model," *IEEE Trans. Veh. Technol.*, vol. 40, no. 2, pp. 472–482, May 1991.

[9] A. Sheikh, M. Abdi, and M. Handforth, "Indoor mobile radio channel at 946 MHz: Measurements and modeling," in *Proc. IEEE VTC'93*, Secaucus, NJ, USA, May 1993, pp. 73–76.

[10] A. Ghasemi and E. S. Sousa, "Opportunistic spectrum access in fading channels through collaborative sensing," *J. Commun.*, vol. 2, no. 2, pp. 71–82, Mar. 2007.

[11] F. F. Digham, M.-S. Alouini, and M. K. Simon, "On the energy detection of unknown signals over fading channels," *IEEE Trans. Commun.*, vol. 55, no. 1, pp. 21–24, Jan. 2007.

[12] I. S. Gradshteyn and I. M. Ryzhik, *Table of Integrals, Series, and Products*, 7th ed. Academic Press, 2007.

[13] H. Shin and J. H. Lee, "On the error probability of binary and M-ary signals in Nakagami-m fading channels," *IEEE Trans. Commun.*, vol. 52, no. 4, pp. 536–539, Apr. 2004.